Supplement of Clim. Past, 22, 2015–2030, 2026
https://doi.org/10.5194/cp-22-2015-2026-supplement
© Author(s) 2026. CC BY 4.0 License.



Climate of the Past
Open Access
EGU

Supplement of

Tree-ring cellulose oxygen isotope reveals summer hydroclimate variability across the East European Plain

Qiaoyun Lin et al.

Correspondence to: Chenxi Xu (cxxu@mail.iggcas.ac.cn) and Wenling An (wlan@mail.iggcas.ac.cn)

The copyright of individual parts of the supplement might differ from the article licence.

Supplementary material

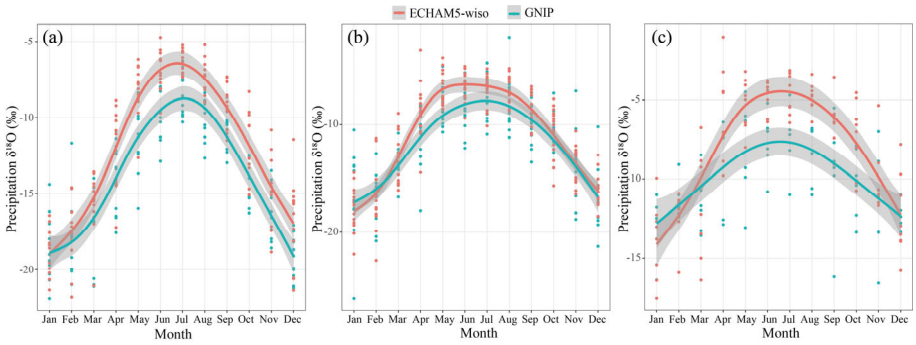


Figure S1. Comparison of the seasonal cycle of precipitation $\delta^{18}O_p$ between ECHAM5-wiso simulations and GNIP observations for overlapping years. Panels (a), (b), and (c) show the northern, central, and southern sites, respectively. The GNIP record periods used for each site are listed in Table S2.

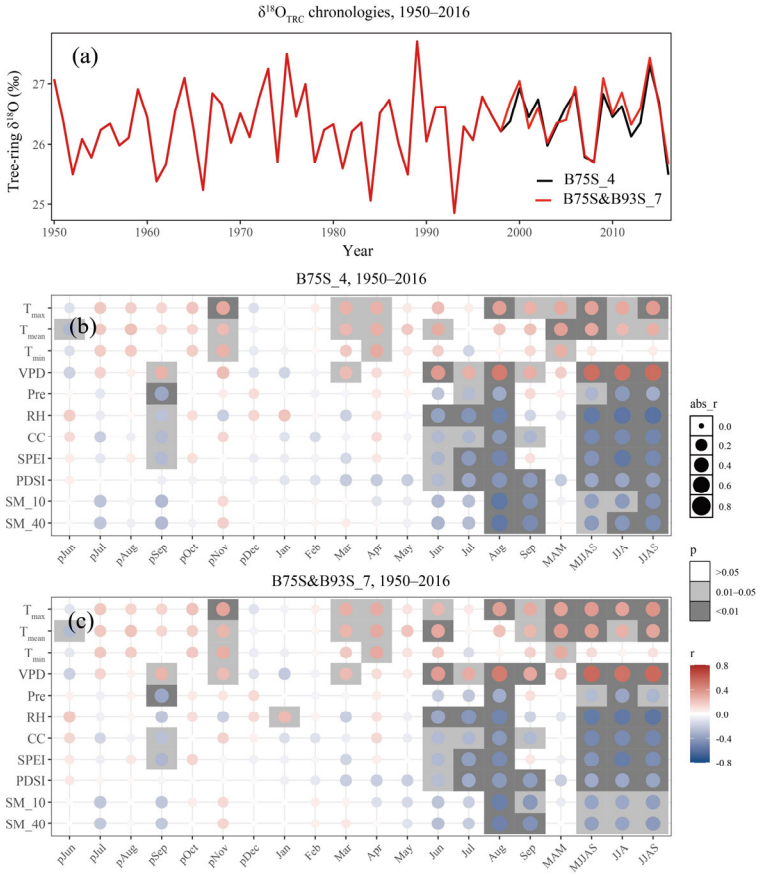


Figure S2. Comparison of the original and expanded northern $\delta^{18}O_{TRC}$ chronologies and their climate responses. (a) Comparison between the original four-tree chronology (B75S_4) and the expanded seven-tree chronology (B75S&B93S_7); correlations between climate variables and (b) the original four-tree $\delta^{18}O_{TRC}$ chronology and (c) the expanded seven-tree $\delta^{18}O_{TRC}$ chronology.

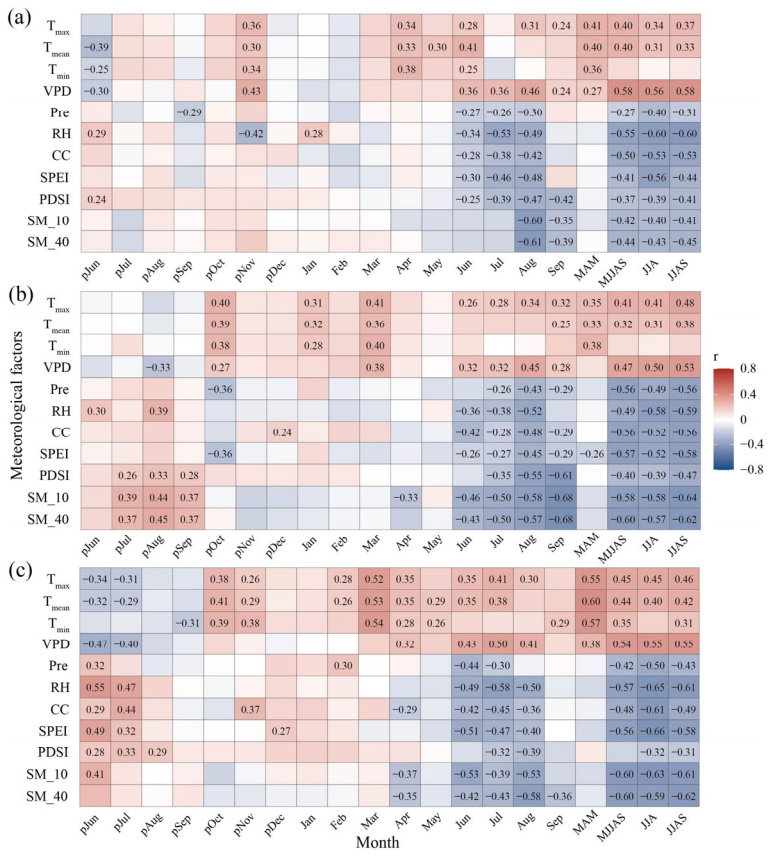


Figure S3. Correlations between first-differenced $\delta^{18}O_{TRC}$ and meteorological factors for the northern (a), central (b), and southern (c) sites in the East European Plain. Time periods and data sources are the same as in Fig. 3, except that the series begin in 1951 and the SM series begin in 1983. Numbers shown in the figure indicate correlations significant at $p < 0.05$.

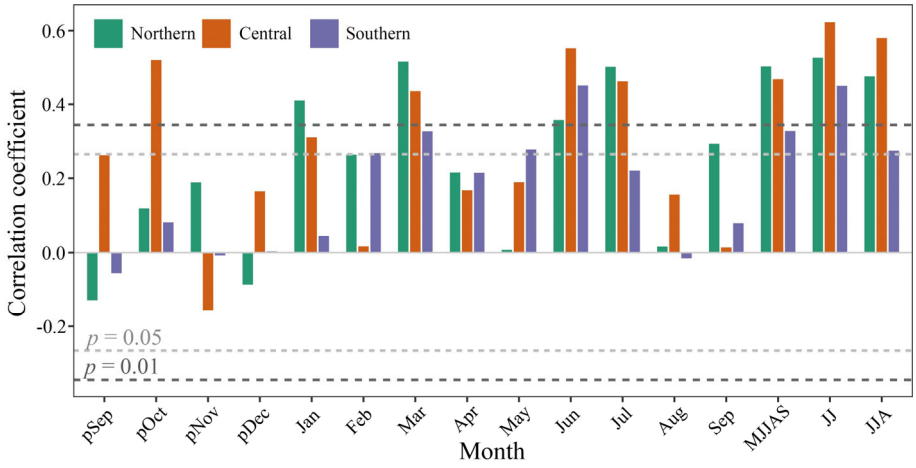


Figure S4. Correlations between first-differenced $\delta^{18}O_{TRC}$ and first-differenced $\delta^{18}O_P$ (1959–2013).

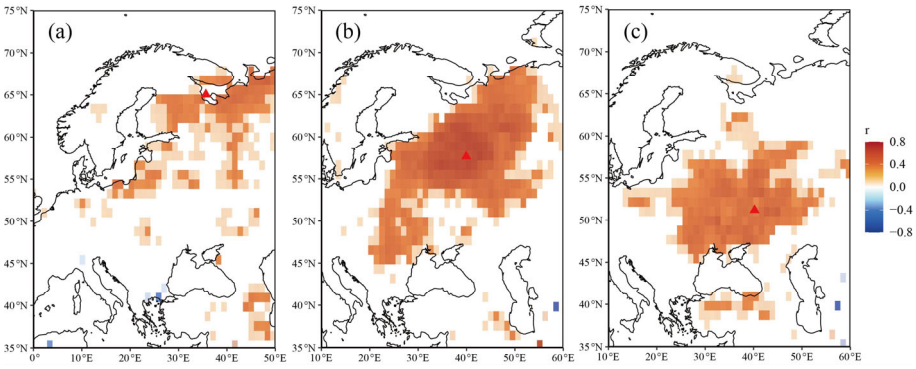


Figure S5. Spatial correlations between $\delta^{18}O_{TRC}$ and ECHAM5-wiso-simulated $\delta^{18}O_p$ (1958–2013) during June–July. Panels (a), (b), and (c) represent the northern, central, and southern sites, respectively.

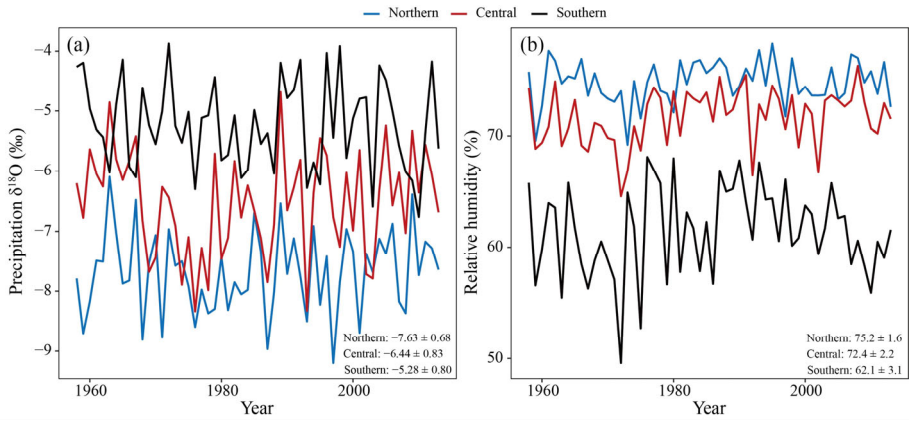


Figure S6. Comparisons of May–September (1958–2013) ECHAM5-wiso $\delta^{18}O_p$ (a), and RH (b) across the three sites. The lower-right corner shows the mean ± SD.

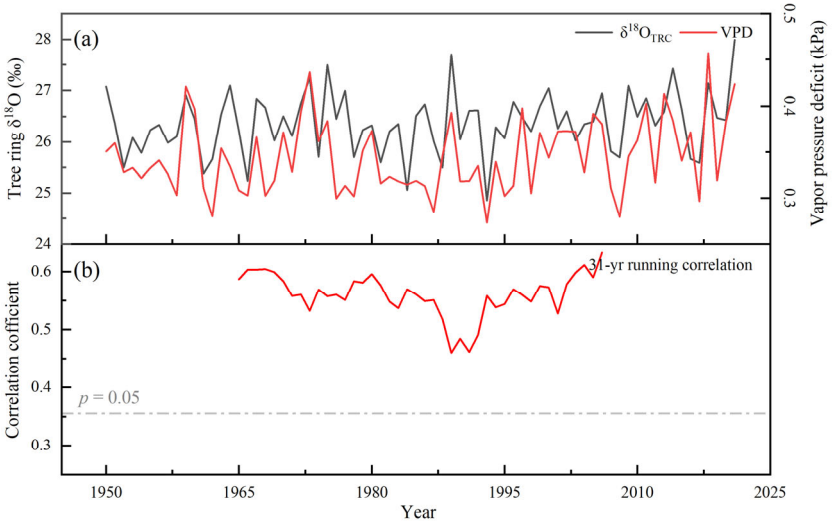


Figure S7. Comparison curves (a) and 31-year running correlations (b) between $\delta^{18}O_{TRC}$ and May–September VPD in the northern region.

Table S1. Numbers of candidate trees and cores available, and cores selected for $\delta^{18}O_{TRC}$ analysis at each study site.

Site	Candidate trees	Candidate cores	Selected cores
Northern—B75S	21	42	4
Northern—B93S	18	36	3
Central—A22S	16	30	4
Southern—T03S	21	36	4

B75S, B93S, A22S, and T03S are sample codes. B93S denotes the additional samples collected during the 2021 resampling campaign at the northern site.

Table S2. Target sites, the grid-center coordinates and bounds for ECHAM5-wiso-simulated $\delta^{18}O_p$, and GNIP stations with their coordinates and record periods.

Site	ECHAM5-wiso	GNIP
North	Target coordinates: 35.641° E, 65.039° N Nearest Grid Centre: 34.875° E, 64.485° N Grid cell range: 34.312-35.438° E, 63.925-65.046° N	KANDALAKSA: 32.35° E, 67.15° N (1996-2000) ARKHANGELSK: 40.5° E, 64.58° N (1980-1986)
Central	Target coordinates: 39.932° E, 57.647° N Nearest Grid Centre: 39.375° E, 57.757° N Grid cell range: 38.812-39.938° E, 57.196-58.317° N	KALININ: 35.9° E, 56.9° N (1980-1988) MOSCOW: 37.57° E, 55.75° N (1970, 1975-1979)
South	Target coordinates: 40.199° E, 51.201° N Nearest Grid Centre: 40.500° E, 51.028° N Grid cell range: 39.938-41.062° E, 50.467-51.588° N	KURSK: 36.27° E, 51.73° N (1996-2000) TAMBOV: 41.47° E, 52.73° N (1980, 1982, 1983)

Table S3. Pairwise correlations among individual $\delta^{18}O_{TRC}$ series from the northern, central, and southern East European Plain. At the northern site, tree cores numbered B93S and B75S were measured for 2000–2021 and 1950–2016, respectively; the tree cores at the central site (A22S) and the southern site (T03S) were measured for 1950–2020 and 1950–2014, respectively. Due to factors such as measurement accuracy and insufficient sample quantity, data may be missing for individual years in different tree cores.

North	B93S7B	B93S17B	B93S9A	B75S4A	B75S11B	B75S19B	B75S12A
B93S7B	1						
B93S17B	0.65	1					
B93S9A	0.56	0.49	1				
B75S4A	0.38	-0.19	0.42	1			
B75S11B	0.64	0.67	0.60	0.59	1		
B75S19B	0.51	0.41	0.74	0.69	0.67	1	
B75S12A	0.61	0.40	0.79	0.55	0.71	0.81	1
North_mean	0.84	0.79	0.81	0.79	0.87	0.89	0.87

Central	A22S11A	A22S12B	A22S13A	A22S16B
A22S11A	1			
A22S12B	0.60	1		
A22S13A	0.56	0.36	1	
A22S16B	0.58	0.58	0.63	1
Central_mean	0.84	0.76	0.81	0.84

South	T03S11B	T03S3A	T03S9A	T03S7B
T03S11B	1			
T03S3A	0.52	1		
T03S9A	0.51	0.47	1	
T03S7B	0.63	0.70	0.53	1
South_mean	0.80	0.81	0.81	0.85

Table S4. Correlation coefficients between the northern $\delta^{18}O_{TRC}$ chronology and monthly/seasonal climate variables.

North	T_{mean}	T_{max}	T_{min}	VPD	CC	Pre	RH	SPEI	PDSI	SM_10	SM_40
pJun											
pJul											
pAug											
pSep				0.245*	-0.292*	-0.269*					
pOct		0.242*	0.238*								
pNov	0.314**	0.382**	0.347**	0.291*							
pDec											
Jan							0.309**				
Feb											
Mar											
Apr	0.357**	0.334**	0.341**								
May	0.268*										
Jun	0.394**	0.337**	0.282*	0.424**	-0.308**		-0.381**	-0.268*			
Jul				0.386**	-0.344**		-0.488**	-0.420**	-0.310**		
Aug		0.336**		0.444**	-0.398**	-0.286*	-0.457**	-0.478**	-0.380**	-0.518**	-0.516**
Sep	0.239*	0.266*		0.298*	-0.293*				-0.376**	-0.483**	-0.507**
MAM	0.372**	0.362**	0.296*	0.241*							
MJJAS	0.415**	0.437**		0.607**	-0.531**	-0.298*	-0.564**	-0.460**	-0.304**	-0.417**	-0.439**
JJA	0.359**	0.413**		0.583**	-0.508**	-0.362**	-0.586**	-0.546**	-0.313**	-0.383*	-0.404**
JJAS	0.382**	0.442**		0.605**	-0.530**	-0.318**	-0.602**	-0.474**	-0.334**	-0.427**	-0.451**

* and ** denote significance levels of $p < 0.05$ and $p < 0.01$, respectively.

Table S5. Correlation coefficients between the central $\delta^{18}O_{TRC}$ chronology and monthly/seasonal climate variables.

Central	T_{mean}	T_{max}	T_{min}	VPD	CC	Pre	RH	SPEI	PDSI	SM_10	SM_40
pJun	0.234*						0.256*				
pJul											
pAug							0.235*				
pSep											
pOct	0.422**	0.433**	0.389**			-0.256*		-0.257*			
pNov											
pDec											
Jan											
Feb					0.262*						
Mar	0.291*	0.320**	0.301*	0.323**							
Apr											
May											
Jun	0.366**	0.355**	0.284*		-0.343**			-0.255*		-0.399**	-0.361*
Jul	0.239*	0.265*		0.253*		-0.236*	-0.259**		-0.265*	-0.407*	-0.414**
Aug	0.263*	0.312**		0.357**	-0.332**	-0.281*	-0.368**	-0.290*	-0.374*	-0.365*	-0.374*
Sep									-0.368**	-0.392*	-0.400*
MAM	0.312**	0.295*	0.297*								
MJJAS	0.393*	0.395**	0.267*	0.321**	-0.383**	-0.413**		-0.420**	-0.283**	-0.383*	-0.404*
JJA	0.412*	0.437**	0.243*	0.380**	-0.380**	-0.395**	-0.335**	-0.402**	-0.292*	-0.433**	-0.422**
JJAS	0.443*	0.451**	0.307**	0.378**	-0.372**	-0.406**	-0.301*	-0.419**	-0.316**	-0.437**	-0.429**

* and ** denote significance levels of $p < 0.05$ and $p < 0.01$, respectively.

Table S6. Correlation coefficients between the southern $\delta^{18}O_{TRC}$ chronology and monthly/seasonal climate variables.

South	T_{mean}	T_{max}	T_{min}	VPD	CC	Pre	RH	SPEI	PDSI	SM_10	SM_40
pJun				-0.280*			0.308*				
pJul											
pAug											
pSep			-0.293*								
pOct	0.326**	0.289*	0.279*								
pNov		0.245*	0.255*								
pDec											
Jan											
Feb	0.268*	0.246*		-0.251*			0.327**				
Mar	0.428**	0.347**	0.385**								
Apr				0.266*	-0.308*						
May											
Jun				0.292*	-0.488*	-0.370**	-0.370**	-0.417**		-0.399*	
Jul	0.344**	0.320**		0.343**	-0.379**		-0.381**	-0.321**			
Aug				0.262*	-0.270*		-0.342**	-0.282*		-0.496**	-0.493**
Sep											-0.380*
MAM	0.417**	0.339**	0.347**								
MJJAS	0.295*	0.298*		0.352**	-0.409**	-0.321**	-0.377**	-0.426**		-0.493**	-0.461**
JJA	0.290*	0.312*		0.370**	-0.480**	-0.314*	-0.452**	-0.508**		-0.479**	-0.431*
JJAS	0.289*	0.301*		0.362**	-0.424**	-0.314*	-0.410**	-0.448**		-0.519**	-0.497**

* and ** denote significance levels of $p < 0.05$ and $p < 0.01$, respectively.

Table S7. Pairwise differences (Δ) in $\delta^{18}O_{TRC}$, observed $\delta^{18}O_p$, RH, and the RH-driven enrichment term (May–September means; NC = North−Central (1980–1983, 1986), CS = Central−South (1980), NS = North−South (1980, 1986, 1996, 1998–2000)).

Pair	$\Delta\delta^{18}O_{TRC}$	$\Delta\delta^{18}O_p$	ΔRH	Δ*E*
NC	–1.290	–0.884	2.753	–0.688
CS	–2.314	–0.22	5.968	–2.243
NS	–4.167	–1.779	12.302	–2.507